RESERVOIR CHARACTERISTICS OF THE COMPLEX KARST OF THE LLUCMAJOR PLATFORM, MALLORCA ISLAND (SPAIN): TOOL FOR HYDROCARBON RESERVOIR APPRAISAL

Philippe A. Lapointe[1]

The development of porosity in carbonate platforms takes many forms. Dissolution porosity as a result of karst processes is unique as it produces organized porosity and permeability over a variety of scales, and can do so in very short periods of time, geologically speaking. Karst developed in the Miocene formations of the Mallorca Island exhibits a complexity that seems to be very similar to the Kashagan or Aktote (Kazakhstan) or Kharyaga (CIS) karst reservoirs architecture characterized by different phases of island karst (mixing water) type with caves of different sizes and sponge karst, reworked and partly filled by paleosoils related to plateau karst developed during major sea level drops and finally hydro- (geo)-thermal processes. The Miocene rocks of the Llucmajor platform in the southwest of Mallorca island exhibit the three main types of karst developments that occurred through time, linked or not to glacio-eustatic changes: -1 Island karst (the flank-margin model); -2 Meteoric karst; -3 Hydrothermal karst/ These developments allow defining the so-called Complex Karst. Each of the terms is identified by specific overprints found in drilled wells (logs and cores) or on outcrops. The outcrops and subcrops of Mallorca Island represent an excellent analogue for understanding the complexity of the past carbonate platforms which are hydrocarbon targets for the industry.

LOCATION

Reef-rimmed prograding platforms were widespread in the western Mediterranean during the Late Miocene (Esteban, 1979). The study area is located south-east of Mallorca, on the Late Miocene Llucmajor platform, which is 20 km wide and up to 200 m thick (Esteban, 1979; Pomar et al., 1983) (Fig. 1). The Llucmajor platform was formed from the Late Burdigalian to Early Messinian. The depositional sequences are characterized by a shallowing-upward trend, with alternating phases of progradation and aggradation related to sea-level fluctuations.

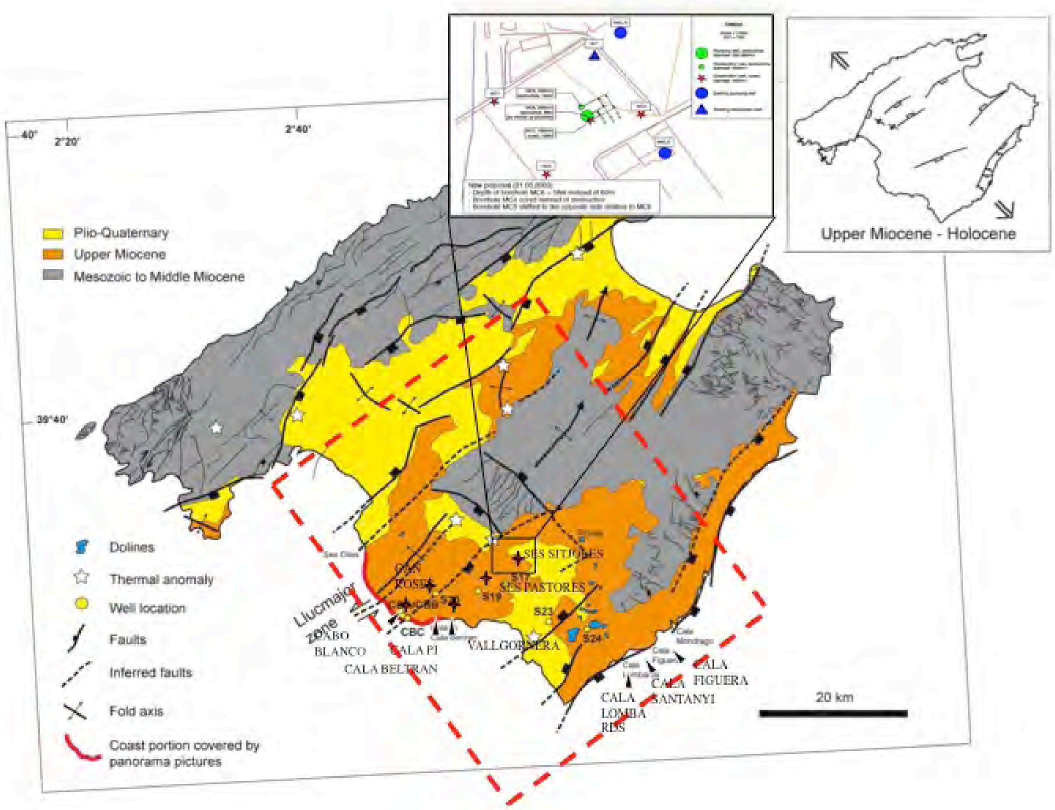

Figure 1. General geological map and location of study area

[1]lapointe-philippe@orange.fr

GEOLOGY OVERVIEW

The Upper Miocene layers are fairly flat-lying limestones and dolostones, and have undergone only slight tilting and flexure associated with normal and strike-slip faulting during Late Neogene to Middle Pleistocene times. Our approach to the Miocene carbonate systems is based on the study of outcrops and new drill cores that have been carried out in the framework of two programs: the "ISES-Shell" Program (J. Kenter coord. unpublished) and the "ALIANCE" Program (Ph. Pézard coord. 2007). The rocks are composed of three major sedimentary units that correspond to third-order depositional sequences (Pomar and Ward, 1994; Pomar et al., 1996; Pomar et al., 2004) with:

- Lower sequence (Early Tortonian): carbonate ramp, including Heterostegina calcisiltites and rhodalgal lithofacies without coral reefs;
- Middle sequence (Late Tortonian – Early Messinian): well-developed progradational reefal platforms;
- Upper sequence (Messinian): variety of lithologies including oolites and stromatolites.

HYDROLOGY

The Llucmajor platform contains a fresh water reservoir affected by an extensive seawater intrusion (Maria-Sube, 2008). At the Campos site, located ~7 km inland, about 20 m of brackish water overlies the salt water. In between, a ~17-m-thick diffusion zone is observed (mixing of fresh and salt water). Four hydrological zones can be distinguished from top to bottom: 1) vadose zone with meteoric water percolation, 2) brackish zone, 3) transition zone and 4) sea water zone (Hebert, 2011). Hydrothermal water corresponding to a deep seated aquifer recharged by fresh water infiltration on the western side of Mallorca flows to the surface through thermal spring (Garcia et al., 2012).

KARST SYSTEM

The limestone consists of a mixture of aragonite, high- and low-magnesium calcite, pure calcite and dolomite, minerals highly reactive on the fluid composition, the calcite and magnesium concentration, the salinity, and the pH. According to the type of fluid-rock interactions, post-deposition diagenesis includes: cementation, dissolution, dolomitization, compaction and recrystallization (Moore, 1989). The overall result is a complex karst system. The main objective was to study a complex karst system analog for application to Kaszakhstan and other karstic petroleum reservoirs. The karst developed in the Miocene formations of Mallorca Island exhibits a complexity looking very similar to the Kashagan and Aktote Karst reservoir complexity with different phases of island karst (mixing water) type with caves of different sizes and sponge karst, reworked and partly filled by plateau karst developed during major sea level drops and finally hydro (geo) thermal karst.

Database

Outcrops - The rather flat and low topography in southern Mallorca implies that the Miocene carbonate platform deposits crop out along cliffs on the coastline. These coastal outcrops include Badia Blava, Cabo Blanco, (Cap de Paret d'Es) Puig des Ros, Cala Beltran, Cala Blava, Cala Figuera, Cala Lombards, Cala Pi, Cala Santanyi, Cala Vallgornera, Portals Vells, and Porto Pi.

Drill cores - The southern part of the Llucmajor Platform (Fig.1) was drilled at Cabo Blanco and in the Can Roses area (S20 core). The Campos Basin was drilled in several areas, Ses Sitjoles (MC2 and MC10 cores), Ses Pastores (S19 core). The distance between the drilling zones ranges from 4 to 10 km. In the Ses Sitjoles area, the Miocene platform carbonate forms a fresh water reservoir. Twelve 100 m holes were drilled/cored at the Ses Sitjoles site (a 100 m scale square field), located 6 km off the Mediterranean coast and 20 km away from the outcrops and drilled holes of the Cabo Blanco (CBB and CBC cores).

KARSTIC FEATURES

Field work was conducted on Mallorca to characterize the position, dimension, and distribution of megapores in the coastal cliffs of the southern coast. The position of the voids within the stratigraphic framework was established, and the nature of regular porosity, and spongework porosity, between the megapores was documented.

Observation of inaccessible cliffs of the Southern Mallorca coast, accomplished by boat, shows classic Sea Caves at the base of cliffs, tafoni as well as Flank margin caves opened by cliff retreat.

Sea cavse and tafoni are erosion related and do not belong to the karst system. tafoni geomorphology designates a hollow shape rounded several decimeters to several meters, carved by erosion in the coastal carbonates; sea caves, also known as littoral caves, are a type of cave formed primarily by wave action. A sea cave is formed by erosion of a weak zone along e.g. fracture/fissure/parting, etc., in the coastal carbonates.

Observation of small cliffs accessible on the coast or through a cala (term for a small bay or creek in Mediterranean islands) shows typical flank margin caves (*sensu* Mylroie et al., 1990) and sponge karst (*sensu* Baceta et al., 2002, 2007, 2008), collapsed caves (Robledo et al., 2002, Ardila, 2005). Meteoric small caves or meteoric reworking of flank margin caves are characterized by speleothems.

On the outcrops of the Cabo Blanco, Cala Pi and Cala Figuera, a comprehensive project was devised with the quantitative description and mapping of the karst systems performed by J. Mylroie and his team from Mississippi State University. All cave and karst features were individually surveyed by compass and tape, and then were tied into a survey line backed up by GPS waypoints.

At Cala Figuera and Cala Pi, the flank margin caves were identified with simple chambers, to clusters of chambers. Marine flooding of the Cala creates flank margin caves in the Cala walls. Following sea-level fall and erosional retreat of the coastline, Cala walls expose the flank margin caves and their meteoric speleothems. Vertical connection through fractures, enlarged by late meteoric karst, crosscut and rework flank margin caves as well as potential sponge karst. At least two main levels of flank margin caves were identified. Collapses are frequently seen on the coastline of the studied area. They develop between two specific levels the basis corresponding to the first flank margin caves level and the top corresponding to the top Miocene.

At Cala Figuera, the sponge karst exists at different locations, on both sides of the Cala. Its thickness ranges from 1 to 2 m maximum, with a pretty wide distribution of several 100 m^2. This sponge karst develops as a zone with levels of discrete spongy porosity traceable for several 10 to 100 m inboard. It is located around the mixing zone and possibly linked to microbially mediated sulphide activity in a zone of reduced circulation. It has been reworked by recent meteoric karst as evidenced by the presence of recent speleothems and paleosoil fills. Paleosoil consists of clays and silts filling in most of the spongy porosity.

Four drill cores, namely; MC-2, MC-10, S-19, and S-20, were analyzed in detail for sedimentology and karst characterization with emphasis on overall porosity. Dating on oyster shells was performed for comparison with the stratigraphic canvas and assessing the drill cores stratigraphic position with respect to the coastal cross-section and the flank margin caves location. Cavernous levels were identified and related to the present and paleo aquifer level as well as to a mixing water wedge. This methodology allows defining the porosity of the karst system away from major caverns (e.g. metric size).

Hydrothermal caverns are known from cave exploreration and studies. The most famous one is Cova des Pas de Vallgornera. This cave seems to result from different karst-forming processes: coastal karstification (mixing water), meteoric water recharge (meteoric karst), together with a probable basal recharge of hypogenic origin (hydrothermal karst sensu largo; Gines et al., 2008; Merino and Fornos, 2010). The latter is supported by hot water resurgence as the thermal spring at Font Sant, located on a fault plane. It discharges water that is sulphate-rich and

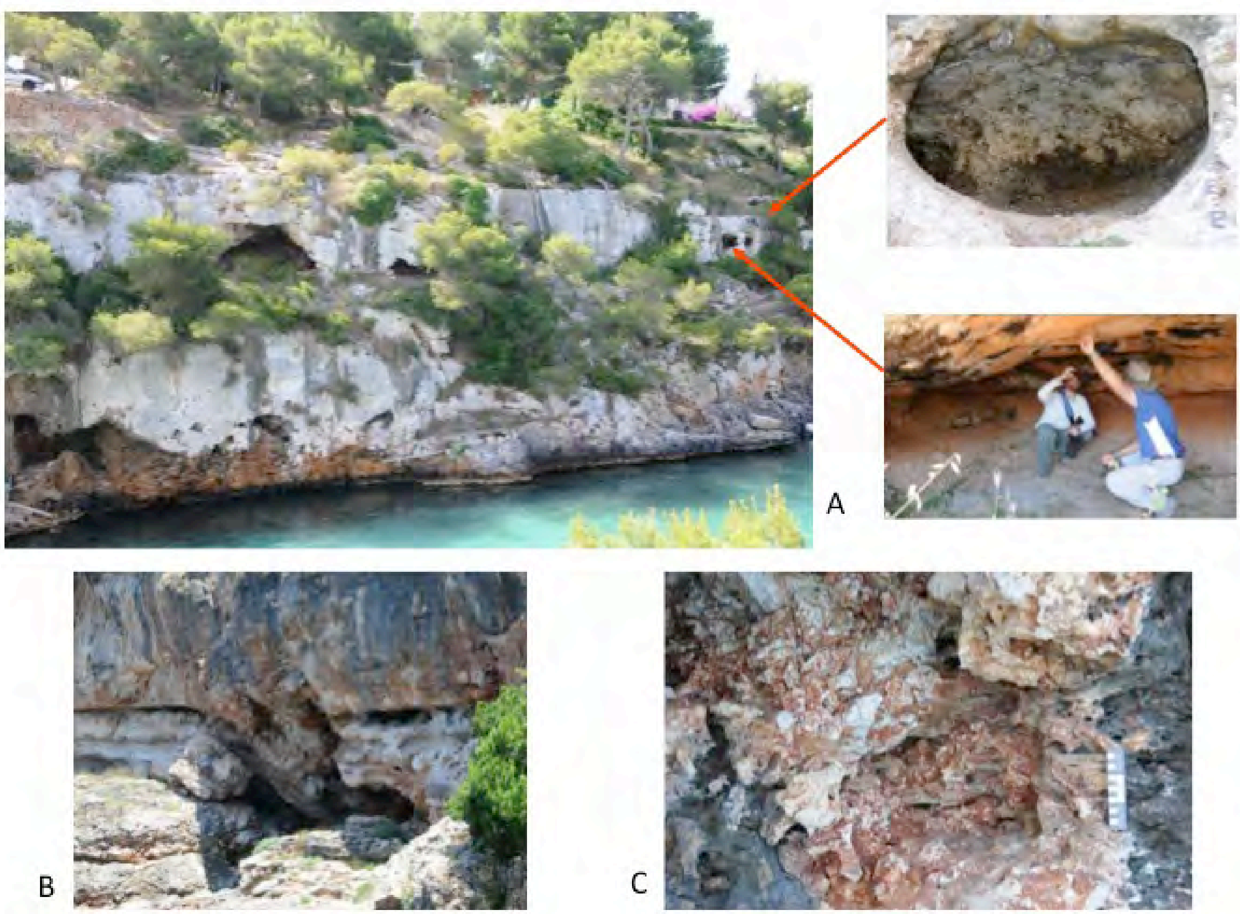

Figure 2. Main karstic features, A) Flank margin caves at Cala Pi, B) Oblique view of a major collapse, 10's m high , Cala Figuera; C) Sponge karst, Cala Bertran.

calcite-rich, with a CO_2 content anomaly and temperature averaging 45-50 °C. Temperatures are in the range of 80-90 °C at 2000m depth (IGME, 2003; Lopez Garcia et al., 2004; Mateos Ruiz et al., 2004).

FAULT AND FRACTURE NETWORK

Mallorca can be considered on the large scale as a horst and graben system that developed across a compressive wedge. NE-SW (N130°) and NW-SE (N50°) structural trends can be interpreted from outcrops as well as satellite imagery in basement and Miocene carbonate platform rocks, and are compatible with the structural trends proposed by Fornos et al. (2012). Thermal anomalies (with hydrothermalism) are rather associated to the NE-SW trending fault trace (N50° trend). Major faults appear to be regularly spaced by 5 to 10 km. The Campos normal fault, trending NE-SW and bounding the Campos basin to the SE, is associated with a thermal anomaly characterized by hot springs known from Roman times at “Font Sant,” about 4 km off the Mediterranean coast. It has been penetrated by a hydrogeological observation hole (S23), intersecting the top of the fault at 14 m (Hebert, 2011). These directions control the development of the Cova Des Pas de Vallgornera. N50° trend is frequently observed as preferential direction for meteoric cave overprint or enlargement of flank margin caves.

POROUS NETWORK QUANTIFICATION – USE OF THE X-RAY COMPUTED TOMOGRAPHY

The CT Scan measures the X-ray density of materials crossed by X-rays. The CT scan image is mathematically reconstructed using the intensities of the transmitted X-ray beam collected at regular increments of rotation around the sample (Ashi, 1997). The intensity of the transmitted X-ray beam is usually expressed as the CT number (Hounsfield scale), i.e., the ratio of the linear attenuation coefficient μ of the material to that of pure water.

Samples

A set of hand specimen collected at Cala Figuera outcrop was analyzed to characterize the porosity in the sponge karst. In order to maximize the results, the hand specimens were cut as cylindrical shapes to provide a better image than an irregular one during acquisition through a medical scanner.

Four wells were selected from the wells cored during the drilling operations conducted by the Bureau of mineral resources of the Mallorca province, namely; MC-2, MC-10, S-19, and S-20. Their respective locations are reported. Along with the CT Scan analyses, a set of conventional core plugs was prepared and measured for calibration.

Virtual Plugging and Virtual Porosity

Virtual plugging consists in sampling a virtual plug of 60 millimetres in length and 39 millimetres in diameter inside the 3D core image. Virtual plugs were taken every 2 centimetres corresponding to 4813 plugs for MC10. With the estimated porosity and X-ray density, a regression curve equation permits to calibrate X-ray density. Using the regression curve equation, virtual porosity can be calibrated, so the curve of virtual porosity of the core can be built every 2 cm using Wellcad©.

Classification of the Porous Network

The next step was to extract and classify the pores by volumetric classes for differentiating, matrix pores, vugs, caverns, etc.; looking for the karst features along the cores. Porosity can be determined by partitioning the voxels (pixel3) belonging to the porosity and the rock matrix using standard image segmentation (Serra, 1982). Density classes are defined by assigning a bin to each grey-level on the image, i.e., determining the grey level range corresponding to pixels having similar properties. The starting point was the x-ray densities computed and the curve of virtual porosity developed for each wells. A specific calibration for the vacuole sizes was devised using test samples with known sizes and associated volumes measured and computed. Then the virtual porosity computed for each core was continuously analyzed based on the vug sizes calibration.

APPLICATION OF THE RESULTS FOR KARST MODELING

Results

Tafonis represent a relatively negligible porosity as they are on the steep flank of the coastline and prone to filling during the next sedimentary phase. Fractures porosity estimate is related to their frequency and as a general rule porosity is low with a maximum less than 0.05%.

Flank margin caves participate as mega pores to the general karstic porosity. The number of sea level changes identified guides their distribution, the measured shapes and the brackish water wedge onto the salt (marine) water intrusion. As a rule of thumb, it decreases away from the coastline. Collapse structures are generated by cave collapse. The related porosity is low compared to the cave porosity. It is similar to breccia porosity. The equivalent porosity can be computed in a first approach using the results published by Loucks (2007). The number and spacing of the collapses reflect the caves distribution, between 20 to 600 m (Robledo, 2002) on 2 sectors studied on the west of Cabo Blanco and on the Eastern coast. The sponge karst dissolution consists of a network of interconnected pores, generally 1–2 cm in diameter with typically sharp smooth to ragged walls, with residual pits and irregular micro-fissures. The amount of dissolution porosity ranges between 6 and 29%, as estimated by CT scan analyses, the larger percentages being more common where the spongy horizons reach maximum thickness.

Each drill core CT-scanned provides a continuous porosity evaluation with the proper calibration performed on conventional core plugs. The extraction and classification of matrix pores, vugs, caverns, provide a porosity estimate for each class that can be directly used for modeling.

Karst Modeling

Karst Modeling for Flank Margin Caves

As expressed above, flank margin dissolution is linked to the paleo-position of sea level at the border of the platform, leading to the definition of a mixing water zone, between seawater and freshwater. This mixing zone is the field of strong dissolution phenomenon leading to flank margin cave to matrix dissolution creation. Dissolution intensity is the strongest near coastline and decreases inland (Labourdette et al., 2007; Labourdette et al, 2013). Areas of dissolution are simulated using truncated gaussian simulations with a proportion defined by coastline position and exponential law decreasing inland. This flank margin dissolution process is a continuum in the size of dissolution features. Vug size and density are simulated with sequential gaussian simulations with exponential variograms with a correlation coefficient for co-simulation with the distance from coastline. This co-simulation allows developing large vugs or caves near the coastline and smaller vugs inland, with a decreasing density. The equivalent petrophysical properties are analyzed to extract deterministic laws linking geometrical properties, porosity and permeability. As for porosity, direct links between permeability and vug density have been found.

Karst Conduits Modeling

This modeling approach leads to horizontally-driven and vertically-driven cave development controlled by all the existing heterogeneities. The resulting complex reservoir is unique and its modeling is achieved through specific geomodeling tools that were internally developed within Total. The software copes with the karst distribution and takes in to account the geological uncertainty associated to that model (Labourdette et al., 2007; Labourdette and Lapointe, 2012; Labourdette et al., 2013; Lapointe and Massonnat, 2008). Conduits are drawn stochastically, crossing the cells of the models. The structural or fracture network is taken into account to generate vertical conduits. The matrix permeability is used to generate horizontal conduit branches. For hydrothermal karst, stochastic seeds are simulated in a defined infiltration zone (base of major stratigraphic layers), at the intersection with the defined fracture network. Vertical conduits are aligned on the fractures. Horizontal conduits are generated when matrix permeability is higher than a defined threshold.

Karst Conduit Petrophysical Properties

Karst conduits are represented in the model as a set of tubes crossing a given cell from one face to the other. During the simulation, conduit radius and conduit number per cells are stored. From these values and cell faces surfaces, equivalent petrophysical properties are calculated using Poiseuille & Darcy's derived laws. The impact of conduits on permeabilities is very strong. Even very small conduits can generate high permeability values; on the contrary, the impact on porosity is weak.

Diffusive Karst Simulation

In the previously defined possible karstified region, the software simulated conduits and associated petrophysical properties. Around these stochastic conduits, an area affected by diffuse karst (matrix dissolution) is defined. Petrophysical properties are simulated in this region, using Gaussian simulations. The permeability is simulated collocated to porosity values with a correlation coefficient.

CONCLUSIONS

Carbonate karst-controlled reservoirs are economically interesting. Mapping of the actual reservoir remains critical for predicting the best porosity-permeability zone distribution and the prognosis of future production well locations, particularly for horizontal or highly deviated wells. The karst modeling workflow applied on actual oil field is supported by the parameters deduced from the outcrop studies of the Llucmajor platform that provide a mandatory set of data. The data set comprises the distribution and sizes of the large caves (flank margin caves, hydrothermal and meteoric caves), the distribution of the sponge karst type with respect to flank margin caves, and its related porosity. The evaluation of the porosity for the diffusive karst as derived from the CT-Scan analysis of the cores.

The 3-D approach leads to horizontally-driven and vertically-driven cave development controlled by all the existing heterogeneities and particularly those related to the tectonic events. The resulting complex reservoir is specific. Its identification and understanding are of paramount importance for reservoir development, particularly in Paleozoic rocks.

ACKNOWLEDGEMENTS

The author thanks the participants in the various field works in Mallorca, Professor J.I. Baceta (University of Bilbao) and Dr. V. P. Wright (Consultant) for the fruitful discussions, R. Lasnel (Total) for the inventive processes analyzing X-Ray tomography, Dr. R. Labourdette (Total) for the introduction to karst modeling, Dr G. Camoin (Cerege) for the sedimentologic analyses and Professor J. Mylroie and his team (Mississippi State University) and Dr P.J. Moore (ExxonMobil) and Dr. J. Bova (Noble Energy).

REFERENCES

ALIANCE (Advanced Logging Investigations of Aquifers iN Coastal Environments), Ph. Pézard coord., 2007, Final Scientific Report, 374p.Ashi, Y., 1997. 11. CT Scan analysis of sediments from Leg 156. Shipley, T.H., Ogawa, Y., Blum, P., and Bahr, J.M. (Eds.), 1997, Proceedings of the Ocean Drilling Program, Scientific Results, Vol. 156.

Baceta J.I., Wright V.P., Pujalte V. 2001. Palaeo-mixing zone karst features from Palaeocene carbonates of north Spain: criteria for recognizing a potentially widespread but rarely documented diagenetic system. Sedimentary Geology, 139: 205–216.

Baceta J.I., Wright V.P., Beavington-Penney S.J., Pujalte V. 2007. Palaeohydrogeological control of palaeokarst macro-porosity genesis during a major sea-level lowstand: Danian of the Urbasa–Andia plateau, Navarra, North Spain. Sedimentary Geology, 199: 141–169.

Baceta J.I., Wright V.P., Pujalte V. Lapointe P. 2008. Eogenetic karstification and palaeohydrology of a Danian land-attached carbonate shelf (North Spain). In: I.D. Sasowsky, C.T. Feazel, J.E. Mylroie, A.N. Palmer, M.V. Palmer (Eds.). Karst from Recent to Reservoirs: International conference on paleokarst & multi-permeability flow systems, Rapid City, South Dakota, USA, 221p.

Esteban M. 1979. Significance of the upper Miocene reefs in the Western Mediterranean: Paleography, Palaeoclimatology, Palaeoecology, 29: 169-188.

Fornós J.J. 1998. Karst collapse phenomena in the Upper Miocene of Mallorca (Balearic Islands, Western Mediterranean). Acta Geologica Hungarica, 42 (2): 237-250.

Fornós J.J., Gelabert B., Ginés A., Ginés J., Tuccimei P., VesicaGarcia P. 2002. Phreatic overgrowths on speleothems: a useful tool in structural geology in littoral karstic landscapes. The example of eastern Mallorca (Balearic Islands), Geodinamica Acta 15.

Ginés J., Ginés A., Fornós J.J., Gràcia F., Merino A. 2008. Noves observacions sobre l'espeleogènesi en el Migjorn de Mallorca: els condicionants litològics en alguns grans sistemes subterranis litorals. Endins, 32:49-79.

Hebert V.2011. Analyse multi-échelle de la structure d'un réservoir carbonaté littoral : exemple de la plate-forme de Llucmajor (Majorque, Espagne), Ph.D Thesis (unpublished results). Université de Montpellier 2, France.

IGME. 2003. Investigación Geotérmica En La Isla De Mallorca, unpublished report, 167 p.

Labourdette R., Lapointe P.A. 2012. Assessing karstic network petrophysics lessons learned from analogue studies example from thermal Pal-Volgy Karst system (Hungary), AAPG Annual Meeting, Long Beach, April 2012.

Labourdette R., Lapointe P.A., Glass L.W. 2013. Nested Karst Simulations and Uncertainty Quantification - Application Case Study from a Kazakhstan Field, SPE Paper 165993, SPE Reservoir Characterisation and Simulation Conference and Exhibition held in Abu Dhabi, UAE, 16–18 September 2013.

Labourdette R., Lascu I., Mylroie J., Roth M. 2007. Process-like modeling of flank-margin caves: From genesis to burial evolution. Journal of Sedimentary Research, 77:965-979.

Lapointe P.A., Massonnat G. 2008. Complex karst-controlled reservoirs - Identification and prediction in 3D-space of reservoir characteristics. In: I.D. Sasowsky, C.T. Feazel, J.E. Mylroie, A.N. Palmer, M.V. Palmer (Eds.). Karst from Recent to Reservoirs: International conference on paleokarst & multi-permeability flow systems, Rapid City, South Dakota, USA, 221p.

Lopez Garcia J.M., Mateos Ruiz R.M., Ballester Rodriguez A. 2004. Aportaciones del sondeo de investigacion geotermica Luis Moragues al modelo de Funcionamiento hidrogeologico de las aguas termales de la plataforma de llucmajor (Mallorca). VIII Simposio de Hidrogeología, pp. 379-388.

Loucks R.G., 1999. Paleocave carbonate reservoirs: origins, burial depth modifications, spatial complexity and reservoir implications. Am. Assoc. Pet. Geol. Bull., 83: 1795–1834.

Loucks R.G. 2007. A Review of coalesced, collapsed-paleocave systems and associated suprastratal deformation. Acta Carsologica, 36(1): 121-132

Mateos Ruiz R.M., Lopez Garcia J.M., Sanchez Guzman J. 2004. Caracteristicas hidrogeoquimicas de las aguas termales de la zona se Lluvmajor (Mallorca), VIII Simposio de Hidrogeología, pp. 399-410.

Maria-Sube Y. 2008. Structure et hétérogénéité d'un récif coralien du Miocène et implication pour les intrusions d'eau salée en zone côtière à Majorque, Espagne. Ph.D Thesis (unpublished results). Université de Montpellier 2, France.

Merino A., Fornos J.J. 2010. Los conjuntos morfológicos de flujo ascendente (morphologic suite of rising flow) en la Cova des Pas de Vallgornera (Llucmajor, Mallorca). Endins, 34: 87-102.

Moore C.H. 1 989. Carbonated diagenesis and porosity. Elsevier, p. 338.

Mylroie J.E., Carew J.L. 1990. The flank margin model for dissolution cave development in carbonate platforms. Earth Surface Processes and Landforms, 15: 413-424.

Mylroie J.E., Carew J.L. 1995. Karst development on carbonate islands. In: D.A. Budd, A.H. Saller, P.M. Harris (Eds.).Unconformities and Porosity in Carbonate Strata. American Association of Petroleum Geologists, pp. 55-76.

Pomar L., Esteban M., Calvet F., Baron A. 1983. La unidad arrecifal del mioceno superior de Mallorca, el terciario de las Baleares (Mallorca-Menorca). Guida de las Excursiones and Congresso Nacional de Sedimentologia, Grupo Espanol de Sedimentologia, p. 139-175.

Pomar L., Ward W.C. 1999. Reservoir-scale heterogeneity in depositional packages and diagenetic patterns on a reef-rimmed platform, Upper Miocene, Mallorca, Spain. AAPG Bulletin, 83: 1759-1773.

Pomar L., Ward W.C., Green D.G. 1996. Upper Miocene reef complex of the Llucmajor area, Majorca, Spain, SEPM Concepts in Sedimentology and Paleontology.

Pomar L., Brandano M., Westphal H. 2004. Environmental factors influencing skeletal grain sediment associations: a critical review of Miocene examples from the western Mediterranean. Sedimentology, 51: 627–651.

Robledo P., Duran J.J., Gumiel P. 2002. Aplicacion del analisis fractal a las paleostructuras de colapso karstico del Mioceno superior de la costa este de Mallorca, Espana. Geogaceta, 31:27-29.

Robledo-Ardila P.A. 2005. Los Paleocolapsos kársticos en las plataformas carbonatadas del Mioceno superior de Mallorca: análisis geográfico, genético, geológico y evolutivo, Universitat de les Illes Balears, PhD Thesis, 307p.

Robledo-Ardila P.A., Durán J.J., and Pomar L. 2004. Paleocollapse structures as geological record for reconstruction of past karst processes during the Upper Miocene of Mallorca Island. International Journal of Speleology, 33 (1/4): 81-94.

Serra J. 1982. Image Analysis and Mathematical Morphology. Acadamic Press, London, pp. 434-463.

Tuccimei P., Ginés J., Delitala M.C., Ginés A., Gràcia F., Fornós J.J., Taddeucci A. 2006. Last interglacial sea level changes in Mallorca island (Western Mediterranean). High precision U-series data from phreatic overgrowths on speleothems. Zeitschrift fur Geomorphologie, 50 (1): 1-21.